



## Research



# Experimental investigation of desiccant dehumidification with four different combinations of silica gel desiccant wheel on indoor air quality

Kishor S. Rambhad<sup>1</sup> · Pramod V. Walke<sup>2</sup> · Vednath P. Kalbande<sup>2</sup> · Manoj A. Kumbhalkar<sup>3</sup> · Vivek W. Khond<sup>2</sup> · Yogesh Nandanwar<sup>2</sup> · Man Mohan<sup>4</sup> · Rahul Jibhakate<sup>2</sup>

Received: 11 July 2023 / Accepted: 25 September 2023

Published online: 03 October 2023

© The Author(s) 2023

## Abstract

Indoor air quality (IAQ) describes the air quality within buildings and other structures, particularly concerning how it affects the health and comfort of building inhabitants. Your likelihood of experiencing indoor health issues can be decreased by being aware of and controlling common indoor contaminants. In addition to maintaining indoor relative humidity at or below 65%, The American Society of Heating, Refrigerating, and Air-Conditioning Engineers (ASHRAE) recommends temperatures between 21 and 26 °C in the summer and 20–24 °C in the winter. The EPA advises using humidity levels between 30 and 60% to stop mold from growing. Silica gel, lithium chloride, and molecular sieves 5A are excellent for dehumidification due to their strong moisture adsorption capability and potential for regeneration. Choosing the right desiccant depends on factors like adsorption capacity, pore size, and chemical compatibility, which are crucial for dehumidification applications and environments. This study compares the performance of silica gel desiccant wheels with three additional composite materials for air dehumidification, which is unusual in this work because very few studies of these combinations have been provided. For all desiccant wheels, the various operating parameters of the needed dehumidification process have been investigated and compared. For adsorption and regeneration rate, the performance of three different composite desiccant wheels was examined and compared experimentally. This experimental evaluation reveals that the composite desiccant wheel (silica gel-lithium chloride-molecular sieve 5A) has a higher adsorption and regeneration rate than others. When a composite desiccant wheel made from silica gel-lithium chloride, silica gel-molecular sieve 5A, and silica gel-lithium chloride-molecular sieve 5A was compared to the performance of a silica gel desiccant wheel, the percentage improvements in adsorption rate were 34.99%, 43.58%, and 85.5%, and the percentage increases in regeneration rate were 5.65%, 7.08%, and 14%.

## Article highlights

- In comparison to other composite desiccant wheels, the one made of silica gel, lithium chloride, and molec-
- ular sieves performs better in all working situations,

✉ Kishor S. Rambhad, kishorsrambhad@gmail.com; Pramod V. Walke, Pramod.walke@raisoni.net; Vednath P. Kalbande, vednathkalbande@gmail.com; Manoj A. Kumbhalkar, manoj.kumbhalkar@rediffmail.com; Vivek W. Khond, vivek.khond@raisoni.net; Yogesh Nandanwar, nandanwar.yogesh@gmail.com; Man Mohan, manmohan.cimt@gmail.com; Rahul Jibhakate, jibhakate.rahu13@gmail.com | <sup>1</sup>Department of Mechanical Engineering, St. John College of Engineering and Management, Palghar 401404, India. <sup>2</sup>Department of Mechanical Engineering, G H Raisoni College of Engineering, Nagpur 440016, India. <sup>3</sup>Department of Mechanical Engineering, JSPM Narhe Technical Campus, Pune 411041, India. <sup>4</sup>Department of Mechanical Engineering, Rungta College of Engineering and Technology, Bhilai, Chhattisgarh, India.



- providing outstanding adsorption and regeneration at 20 rph.
- Contrary to parallel flow arrangements, counterflow arrangements have higher adsorption rates and regeneration rates.

- The average adsorption and regeneration rates of the composite desiccant wheel composed of silica gel, lithium chloride, and molecular sieve 5A were 0.64 kg/h and 1.98 kg/h, respectively.

**Keywords** Composite desiccant wheel · Dehumidification rate · Parabolic trough solar collector · Regeneration rate

#### List of symbols

W	Humidity ratio (kg/kg of dry air)
A	Surface area/cross sectional area ( $m^2$ )
Ar	Area ratio of air flow passage to the total area of one channel (-)
hm	Average heat transfer coefficient between the absorber tube and glass envelope ( $W/m^2 K$ )
pc	Flow passage pitch (mm)
Pe	Perimeter of air flow passage of one channel (m)
RH	Relative humidity (%)
P	Pressure (Pascal)
Ra	Adsorption rate (kg/h)
Rr	Regeneration rate (kg/h)
E	Wheel effectiveness
T	Temperature in ( $^{\circ}C$ )
D	Diameter (mm)
L	Length (mm)
M	Mass flow rate (kg/h)
N	Rotational speed of the desiccant wheel (rph)

#### Abbreviations

PTSC	Parabolic trough solar collector
VCR	Vapor compression refrigeration

#### Subscripts

a	Adsorption sector
r	Regeneration sector
s	Saturation
b	Barometric
c	Channel
w	Wheel
p	Process sector
m	Matrix material

#### Greek symbols

$\rho$	Density ( $kg/m^3$ )
$\delta$	Thickness (mm)

## 1 Introduction

The phrase “indoor air quality” (IAQ) is used to describe the air quality inside buildings and other structures, especially how it impacts the health and comfort of building

occupants. By being aware of and in control of common indoor pollutants, you can lessen your risk of encountering indoor health problems. ASHRAE advises temperatures between 21 and 26 °C in the summer and 20–24 °C in the winter, in addition to keeping indoor relative humidity at or below 65%. The Environmental Protection Agency (EPA) recommends utilizing humidity levels between 30 and 60% to prevent the growth of mold [1].

In the current scenario, the increasing energy demand is a global issue because of the rapid exploitation of conventional energy resources such as petrol, coal, natural gas, etc. The present energy scenario with increased energy demand and associated energy cost needs the use of alternative technologies [2].

In summer air conditioning, traditional vapor compression systems cooled the process air to its dew point temperature for dehumidification and then heat it to the appropriate supply temperature [3, 4]. Desiccant cooling systems have been touted as a viable alternative to traditional domestic air conditioning systems due to their ability to significantly reduce electricity usage. The total efficiency of the system may be greatly improved when they are integrated with distributed power production by using the system exhaust heat for the adsorption of water from the solid desiccant [5, 6].

In recent years successful efforts in the direction of utilizing low-grade thermal energy have been trying to keep the price of crude oil constant up to some extent [7]. In various domestic applications like dehumidification, water extraction, cooling, and air-conditioning purpose, desiccant materials have been proven as a potential supplement to traditional vapor compression refrigeration (VCR) systems [8, 9]. Desiccant dehumidification systems are thermally regenerated systems that may be employed as standalone units or as supplements to standard cooling systems [10]. Desiccant materials have the potential to adsorb/absorb moisture due to differences in vapor pressure and this takes place through chemical reactions. Desiccant materials have also been applied to a wide range of industrial applications area such as medicament storage, nourishment storage, hygroscopic (adsorbent) material storage, etc. [11, 12]. Liquid and solid desiccants are another of its category which is utilized in air drying, air-conditioning, and cooling systems in various arrangements such as packed and fluidized beds and desiccant

wheels [13, 14]. Once thermally regenerated and adequately cooled, solid desiccant is used to remove excess humidity from unsaturated air [15, 16]. The desiccant in conjunction with solar energy can be used to provide suitable supplementary to conventional air-conditioning techniques [17, 18].

In the present energy scenario, composite desiccant materials are showing enough potential with high-effectiveness energy applications. Jia et al. experimentally compared two honeycombed rotary desiccant wheels developed with silica gel and composite desiccant materials, and found a remarkable difference in the performance, due to the presence of haloid salt in the pores of silica gel. Haloids block old pores and create many small new pores [19]. Wrobel et al. reported that the spillover phenomenon does not occur because of its physical structure if the suitable percent of porous host matrix and haloid is provided [14]. Kabeel constructed a honeycomb desiccant wheel using cloth layers and iron wires impregnated with calcium chloride solution, this desiccant wheel has been used for the adsorption process and solar energy was used for the regeneration process [20]. Chen et al. performed the dehumidification of the process air by polymer composite desiccant wheel and silica gel desiccant wheel and used a heat pump to regenerate the desiccant wheel [21, 22]. Tretiak et al. designed and tested a composite desiccant wheel made of calcium chloride and clay for diverse sorption and desorption applications in the adsorption and regeneration industry [23]. Ramzy et al. employed silica gel and a new composite desiccant material in which inert particles are placed in the empty space of a spherical silica gel desiccant material. The pressure drop is reduced by around 60% when this particle with a thickness ratio of 0.2 is used [24]. Chua and Islam suggested that the maximum composition of a hygroscopic substance such as calcium chloride, lithium chloride, and bentonite can be impregnated with approximately 10% of its mass into the pore of silica gel to avoid spillover phenomenon and hence better performance can achieve [25]. Zhang et al. suggested the design of adsorbent beds which are of honeycomb type for water vapor adsorption with various solid desiccant boundary materials such as silica gel RD, silica gel 3A, etc. [26]. Majumdar in 1998 investigated a composite desiccant for dehumidification made of mixed inert and desiccant material, some other researchers also discussed a mode of heat and mass transfer that incorporates the composite nature of the structure [27]. Jia et al. investigated the innovative composite desiccant consisting of a host matrix such as silica gel with open pores and LiCl absorbed into its pores in 2007. When compared to normal silica gel, this test result demonstrates that the innovative composite desiccant wheel can remove roughly 20–30% more moisture from the process air [28]. Zhang et al.

employed calcium chloride, silica gel, and silica gel with calcium chloride on a corrugated paper-based desiccant wheel between 2003 and 2006. The CP-SG-CaCl<sub>2</sub> material was found to achieve equilibrium in a relatively short time, and its hygroscopic capacity is substantially higher than that of CP-SG. It also exhibits a large increase in moisture removal when compared to the SG wheel [29, 30]. Shahrooz Motaghian et al. used an artificial neural network (ANN) approach to forecast the performance of a DW [31]. By impregnating-spraying, Zhongbao Liu et al. produced a new metal-organic framework composite adsorbent desiccant wheel (MOF DW) [32]. Goodarzia et al. have done the performance evaluation of a waste heat-based solid desiccant wheel and found a remarkable rise in the moisture removal capacity of composite material compared with silica gel [33]. Recently Chen et al. and Muzaffar Ali et al. studied a novel desiccant system for cooling and air-conditioning with sustainable regeneration heating and natural cooling source for improved energy efficiency, the exploratory results are approved by their numerical analysis. This novel system could accomplish great cooling and dehumidification with the recovery temperature is 80 °C. Apart from this, the system indicates better execution and supply air at the required temperature and humidity ratio [34, 35].

One more recent study has been developed by Samad et al. on dynamic simulation and parametric analysis of the desiccant cooling system with three different configuration schemes. They used a photovoltaic solar collector for operating a desiccant cooling system. The first configuration employed an auxiliary heater for the heating of return air up to the desired regeneration temperature. The second configuration used the auxiliary heater to raise the temperature of the water to a certain evacuated temperature, whereas, in the third configuration, all the cooling was achieved by a conventional vapor compressor chiller. The simulation results for all configuration schemes estimate that the optimum regeneration temperature occurs between 50 and 70 °C [36].

Fong et al. in the year 2020 developed a solar-assisted desiccant cooling system for hot and humid summer climates. Through this study, three different types of systems have been proposed, i.e., solar absorption chilling (AB), solar absorption chilling with energy recovery unit (AB + ERU), and solar absorption chilling with desiccant cooling system (AB + DCS). AB + ERU offered an 11.5% reduction in primary energy consumption (PEC) and a 9.5% improvement in the solar fraction (SF) as compared to the AB + DCS system [13].

Recently in 2019, Valarezo et al. developed three different and novel composite desiccant-coated heat exchangers using silica gel, silica gel with sodium acetate, and potassium formate with silica gel as a coating material.

In this experiment, the performance of the above three has been compared and it has been concluded that a heat exchanger coated with sodium acetate has an outstanding role for cooling and effectiveness. The dehumidification rate was enhanced by 10% and 30% as compared to potassium formate coated with silica gel and heat exchanger coated with silica gel [37]. Li et al. investigated biomass gasification-based cogeneration systems integrated with desiccant-coated heat exchanger dehumidification, covering the cogeneration system inclusive of sensible heat storage and internal heat recovery (SC-1), the cogeneration system inclusive of sensible heat storage (SC-2), and the cogeneration system exclusive of heat storage and internal heat recovery (SC-3) [38].

One more study in the recent year 2019 done by Vivekh et al., developed three-dimensional mathematical modeling for heat exchangers coated with desiccants. Through this study the mathematical results have been compared with experimental results, the experimental results were obtained from a silica gel coated heat exchanger and composite polymer desiccant. The maximum variation between mathematical and experimental results for outlet air temperature and humidity ratio were  $\pm 14\%$  and  $\pm 12\%$  respectively [39, 40].

For water production from atmospheric air, Shrivastava et al. employed a solar-assisted desiccant wheel. This research used three composite desiccant materials at 37% concentration, including lithium chloride-sand, calcium chloride-sand, and lithium bromide-sand, as well as sand as a host material. To manufacture water from ambient air, the adsorption and desorption processes are alternated. In 5 h and 30 min, 4 h and 30 min, and 4 h and 30 min, respectively, lithium chloride-sand, calcium chloride-sand, and lithium bromide-sand yield 0.090 L per day, 0.115 L per day, and 0.073 L per day [41]. Liu et al. propose a method for gathering atmospheric water that may be powered by renewable heating and cooling sources. It is designed for usage in humid environments. The system employs multistage desiccant wheels to raise the humidity ratio of the processed air before condensing it to collect water [42].

From the above study, it is observed that a composite of Silica gel, Lithium chloride, and Molecular sieves has not been used to generate dry air. Hence the composite of these materials has been taken for the present analysis, moreover, the properties of these materials are favoring dehumidification.

The prime objective of this experiment must fabricate and investigate the experimental performance of four different desiccant wheels. The first desiccant wheel has been made from silica gel and others are being made from composite desiccant material namely silica gel-lithium chloride, silica gel-molecular sieve 5A, and silica gel-lithium chloride-molecular sieve 5A. The present experiment has

been carried out by using a parabolic trough solar collector for the regeneration of the desiccant wheels. The performance of desiccant wheels is investigated and compared for parallel and counter flow arrangement, for various process and regeneration areas, the various rotational speed of the desiccant wheel, the various airflow rate in the process sector and regeneration sector (i.e., the ratio of mass flow rate at regeneration side to process side R/P ratio). Moreover, through these experiments, the objective aimed to achieve is to select the best desiccant material and to obtain the best operating parameters of the same desiccant wheel for air dehumidification in hot and humid conditions anywhere.

Desiccant wheels also referred to as dehumidification wheels or sorption wheels, can regenerate their desiccant materials using a process called solar regeneration. In Heating, Ventilation, and Air Conditioning (HVAC) systems and other applications where dehumidification is crucial, a desiccant wheel is a crucial component [43, 44].

In the present paper, Sect. 2 comprises the requirements of the system viz. desiccant dehumidifier, desiccant wheel, operation of the desiccant dehumidification system, performance indices, etc. Section 3 is the experimental setup; in this section performance parameters of the desiccant wheel are explained. Section 4 is the result which shows the finding of the present work. Section 5 is a discussion in which discussion on the obtained result was made. Section 6 is a validation of experimental and simulation results; this section also shows the comparison and deviation between experimental and simulation results. Section 7 consists of the simulation of the desiccant wheel at various conditions. Section 8 is a Comparison with published work and Sect. 9 is the conclusion.

## 2 Requirement of the system

### 2.1 Desiccant dehumidifier

A desiccant dehumidifier is a stationary or slow-rotating desiccant bed that adsorbs the moisture of process air. The term process air implies the air having moisture of which moisture needs to be removed. Desiccant dehumidifier requires periodic regeneration which can be done by using waste exhaust heat or solar energy [45, 46]. In other words, the rotary desiccant wheel is a periodically regenerated slow-speed desiccant bed that comprises channels of paper or fiberglass at the outer frame of various shapes like a honeycomb, triangular sinusoidal, etc. The entire process takes place in two separate sectors (area) of the wheel, dehumidification of processed air takes place in the process sector of the wheel, and wheel regeneration takes place in the regeneration sector of the wheel [45].

Silica gel can absorb a maximum of 40% moisture of its dry weight as well as can handle temperatures up to 400 °C. Since it is solid insoluble material hence it does not require any special attention even at 100% relative humidity. It is washable and does not undergo any chemical or physical change. It is stable and non-poisonous. It has a very low regeneration temperature ranging from 50 to 120 °C [47]. Molecular sieve 5A is an aluminum silicate that has a crystalline structure. It has the capacity for separating different sizes of water molecules and is suitable for dehumidifying air to a very low humidity ratio [18]. Lithium chloride can absorb ten times the moisture of its dry weight. The chemical reaction involves the process of absorption of water vapor of air into Lithium chloride. Most importantly, it requires proper attention during the absorption process because it is soluble in water. It has a superior characteristic that, it reduces 25–50% of bacteria from the air when air is passed through lithium chloride [48].

## 2.2 Description of the desiccant wheel

Four different desiccant wheels have been fabricated. Desiccant wheels were made from silica gel, silica gel-lithium chloride, silica gel-molecular sieve 5A, and silica gel-lithium chloride-molecular sieve 5A, as would understand from Fig. 1.

**Table 1** Desiccant wheel specifications

Parameters	Quantities
Desiccant wheel diameter, $D_w$ (mm)	500
Desiccant wheel length, $L_w$ (mm)	100
Channel wall thickness, $\delta_c$ (mm)	0.4
Flow passage height of, $h_c$ (mm)	25
Flow passage pitch, $p_c$ (mm)	25
Matrix material density, $\rho_m$ (kg/m <sup>3</sup> )	7850
Matrix material thermal conductivity, $k_m$ (W/m K)	54
Matrix material specific heat, $c_m$ (J/kg K)	465

**Fig. 1** Various desiccant materials



**Table 2** Composition of composite desiccant

Composite desiccant	Composition		
	Silica gel (%)	Lithium chloride (%)	Molecular sieve 5A (%)
Silica gel-lithium chloride	90	10	0
Silica gel-molecular sieve 5A	90	0	10
Silica gel-lithium chloride-molecular sieve 5A	80	10	10

The complete specification of the desiccant wheel is available in Table 1 as well as the composition of composite desiccant is available in Table 2.

All four desiccant wheels were made from silica gel as well as other three composite desiccant materials with 500 mm diameter and 100 mm length (Tables 1, 2). Figure 2 shows a picture of the desiccant wheel assembly.

To enhance the performance of the rotary desiccant wheel, it is made from composite desiccant materials. In total four desiccant wheels are fabricated viz one from silica gel and other three from composite materials. For this study silica gel, lithium chloride, and molecular sieves 5A were selected for many reasons. Silica gel can adsorb up to 40% of its dry weight in water, it can withstand temperatures up to 400 °C, and no special precautions are required when it is exposed to air at 100% relative humidity. It is also possible to wash a wheel in water if dust or another particulate block the air passage, it is inert; Silica gel does not undergo any chemical or physical change during the adsorption process, stable and resistant to most chemicals. It is non-toxic and insoluble desiccant and regeneration temperature is 50–120 °C which is easily achievable. These characteristics make silica gel a favorite in this field. Lithium chloride can attract and hold over ten times its weight in water, Its ability to attract and hold water is due to the absorption of water through a chemical reaction.

**Fig. 2** Desiccant wheel assembly

Lithium chloride is unaffected by most air stream pollutants, and resistant to many contaminants such as petroleum vapor, solvents, etc. It can significantly reduce the number of organisms that may be carried in the air stream. Test results show there is typically a 25–50% reduction in the bacteria content of the air as it passes through the wheel. Molecular sieves 5A are crystalline and highly porous materials, it is used for the desiccation and purification of air, dehydration, and desulphurization of natural gas and liquid petroleum gas, oxygen, and hydrogen production by pressure swing adsorption process. Three composite desiccant wheels were made by combining these materials by adopting proper procedures to check their performance for various parameters.

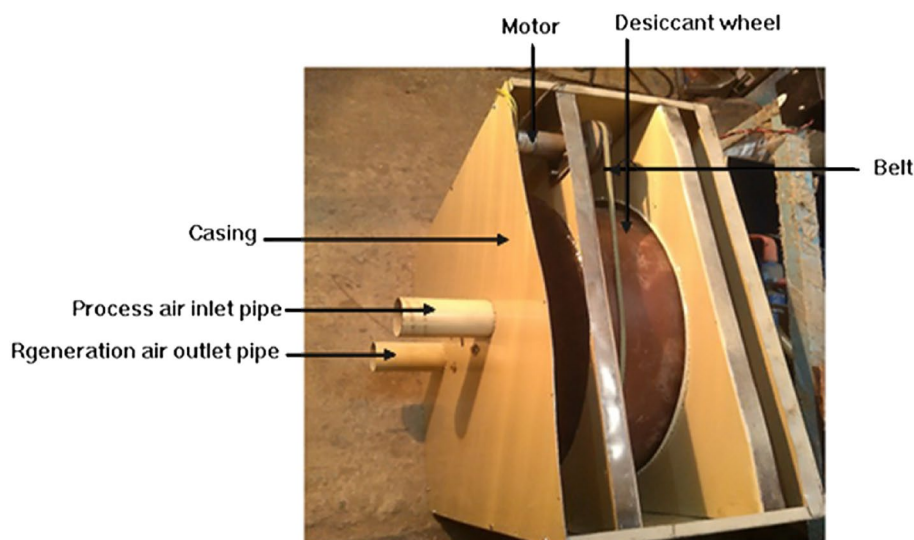
To pass the process air through the desiccant wheels parallel flow channels are provided. In the process area when the desiccant wheel adsorbs moisture, it requires to be regenerated with hot air simultaneously. In the regeneration process, hot air from the parabolic trough solar collector (PTSC) is passed through the regeneration area of the desiccant wheel which removes the moisture adsorbed on the desiccant material. This simultaneous adsorption and regeneration are continuous throughout the working time of the system (Fig. 2).

### 2.3 Operation of the system

The entire process of desiccant dehumidification takes place in three separate processes as described through the psychrometric processes of Fig. 3.

- (i) Process a–b: Sensible heating of regeneration air,
- (ii) Process b–c: Regeneration of desiccant wheel,
- (iii) Process a–d: Dehumidification of process air.

The sensible heating of regeneration air (a–b) is a procedure in which air is heated sensibly for desiccant wheel



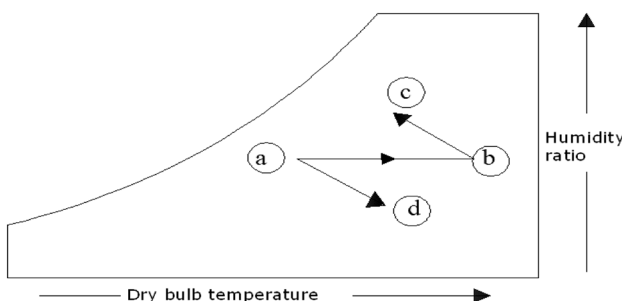


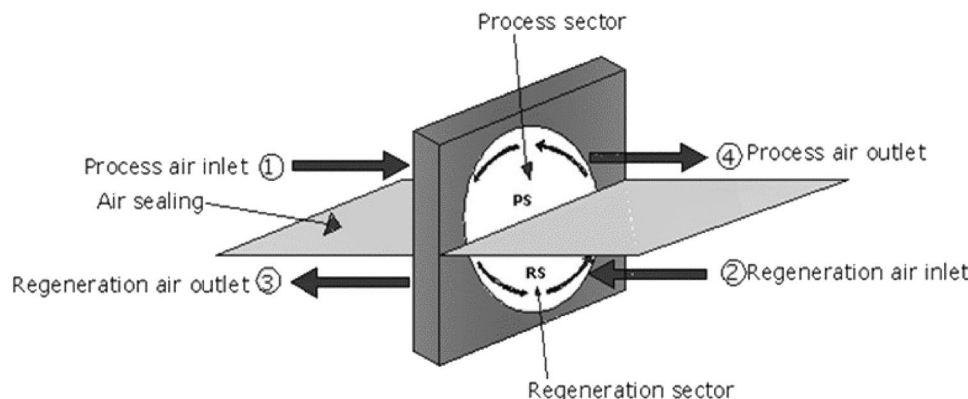
**Fig. 3** Psychrometric processes showing sensible heating, regeneration, and adsorption

renewal using a parabolic trough solar collector. The regeneration of the desiccant wheel (process b–c) takes place in the regeneration area and involves the regeneration of the desiccant wheel using hot air. Hot air removes moisture from desiccant material in this process, losing its temperature in the process. Figure 3 process (a–d) shows the dehumidification of process air by the desiccant wheel, here process air containing moisture flows through the adsorption area and reduces its moisture content. In the dehumidification process (a–d), moisture of process air gets condensed and releases its latent heat which is taken up by dried air as a sensible heat hence the temperature of dried air increases during the dehumidification process.

Figure 4 shows the separation of the adsorption and regeneration sector in which the adsorption sector and regeneration sector are separated by air sealing (air separating plate).

Air sealing prevents the mixing of process and regeneration air in the desiccant wheel. The term PS represents the process sector whereas RS represents the regeneration sector. Process air inlet, regeneration air inlet, regeneration air outlet, and process air outlet are marked with points 1, 2, 3 and 4 respectively.

**Fig. 4** Schematic diagram showing separation of process and regeneration sector



## 2.4 Indices of performance

The study checked the experimental performance of all four desiccant wheels by following relations. The specific per unit of dry air is expressed by Eq. 1.

$$M_{RR} = W_{pi} - W_{po} \quad (1)$$

where  $M_{RR}$  is expressed in kg per kg of dry air,  $W_{pi}$  and  $W_{po}$  are the humidity ratios of the moist air at the inlet and outlet. Equation 2 represents the moist air humidity ratio [7].

$$W = 0.62198 \frac{RH * P_s}{P_b - RH * P_s} \quad (2)$$

$RH$  represents relative humidity of air in percent and  $P_s$  and  $P_b$  represent saturation pressure and barometric pressure in Pascal. The saturation pressure of air is given by Eq. 3 [29].

$$P_s = e^{\left(23.196 - \frac{3816.44}{(T+273)-46.13}\right)} \quad (3)$$

where  $T$  is dry bulb temperature in °C. The adsorption rate of the desiccant wheel is given by Eq. 4 [20].

$$R_a = M_p (W_{pi} - W_{po}) \quad (4)$$

Wheel effectiveness in the adsorption sector is given by below Eq. 5 [20].

$$E_a = \frac{W_{pi} - W_{po}}{W_{pi}} \quad (5)$$

The regeneration rate of the desiccant wheel is given by Eq. 6 [20].

$$R_r = M_r (W_{ro} - W_{ri}) \quad (6)$$

Wheel effectiveness in the regeneration sector was calculated by Eq. 7 [20].

$$E_r = \frac{W_{ro} - W_{ri}}{W_{ri}} \quad (7)$$

Percentage improvement in the adsorption rate of composite desiccant wheels is given by Eq. 8 [22].

$$R_{a\text{composite desiccant wheel}} = \left( \frac{R_{a\text{composite desiccant wheel}} - R_{a\text{silica gel}}}{R_{a\text{silica gel}}} \right) * 100 \quad (8)$$

The percentage improvement in the regeneration rate of the composite desiccant wheel is given by Eq. 9 [22].

$$R_{r\text{composite desiccant wheel}} = \left( \frac{R_{r\text{composite desiccant wheel}} - R_{r\text{silica gel}}}{R_{r\text{silica gel}}} \right) * 100 \quad (9)$$

**Fig. 5** Experimental setup of the system

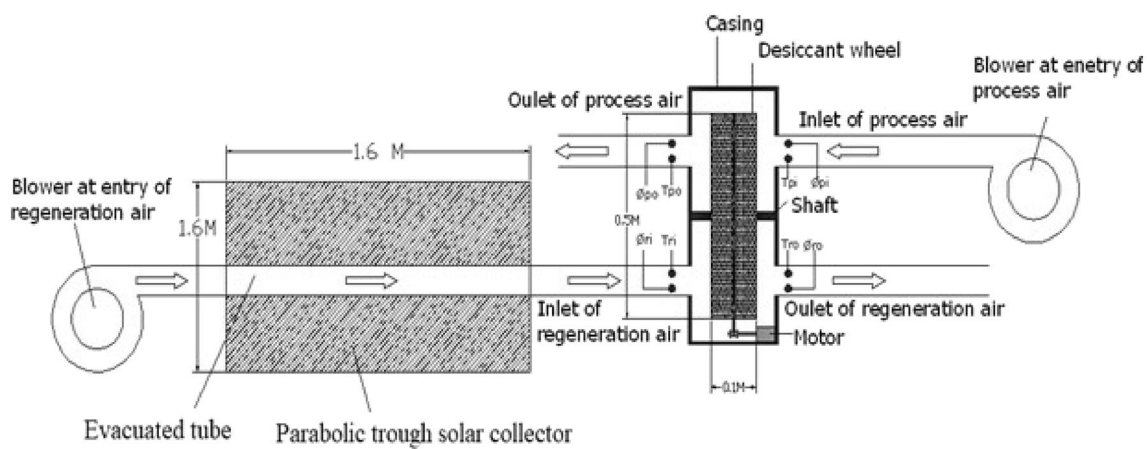


**Fig. 6** Schematic of the experimental setup of the system

### 3 Experimental setup of the system

The experimental facility was fabricated as well as experimentation has been performed. The schematic diagram of this experimental setup of the system is available in Figs. 5 and 6 respectively. Four different rotary desiccant wheels were fabricated through all the indigenous raw materials. The material used for the fabrication of desiccant wheels is silica gel, (silica gel-lithium chloride), (silica gel-molecular sieve 5A), (silica gel-lithium chloride-molecular sieve 5A). The blending of the desiccant material is based on economics, applicability, and performance. Experimentation was performed during the daytime from 09.00 to 17.00 h, inlet temperature and relative humidity of air varied from 25 to 40 °C and 55 to 75%.

The experimentation was repeated several times to get an average reading since maintaining identical experiment conditions for each test is not possible. The desiccant wheel operates on the sorption principle, which is an adsorption mechanism in which a desiccant removes water vapor from the air directly. The air that must be dried flows through the desiccant wheel, which extracts and holds the moisture straight from the air as it rotates. Following that, the hot regeneration air is passed via a moisture-laden desiccant through the regeneration sector, where the moisture is transformed into a hot air stream (regeneration air), which is then vented to the outside, ensuring that PTSC maintains a constant supply of hot air for regeneration. This process makes a loop, allowing for highly effective and uninterrupted dehumidification. The rotary movement to the desiccant wheels is facelifted by using a 12 Volt DC motor. Two different configurations of airflow areas have been adopted to perform this experiment. In the first case with 50% process area and 50% regeneration area whereas in the second case, 75% process area and 25% regeneration area of the wheel have been considered to obtain optimized operating parameters. The experiment has been performed by variation in process and regeneration air

flow rate, the direction of flow (parallel flow and counter flow), and desiccant wheel rotational speed. This experimental setup allows the adsorption and regeneration at the same time i.e., daytime in the availability of solar radiation. Parabolic trough solar collector comprises of mirror reflector and evacuated tube, the aperture length of the collector is 1.6 m, and length of the absorber tube is 1.6 m. The outer and inner glass tube diameter of the absorber tube is 0.058 m and 0.047 m respectively. In this experimental setup, reflector mirrors are used for reflecting solar radiation. Two blowers of 1 HP are used to blow the air; a flow regulator is used to control the airflow rate. To improve regeneration temperature, an aluminum coil was placed inside the evacuated tube. This slow rotation of the wheel facilitates the alteration of the position of the desiccant wheel for the adsorption sector and regeneration sector as shown in Fig. 7 shows the picture of the raw materials of the desiccant wheel used in the present experiment.

The proper care has been taken during air sealing to separate the two sectors of the wheel namely the adsorption sector and regeneration sector. The height and pitch of flow passage of each channel were 25 mm and 25 mm respectively and the thickness of the wall of the channel was 0.4 mm. The desiccant materials are placed and packed inside the channel. DC motor was used to drive the desiccant wheel at the speed of 10, 20, and 30 revolutions per hour (Fig. 7).

### 4 Results

The experimental results of solar-assisted silica gel and composite rotary desiccant wheels were analyzed for various rotational speeds, different types of flow arrangements, same and different sector angles, and different regeneration/process (R/P) ratios under various atmospheric conditions with its specifications given in Table 3. The main objective of this study is to compare the performance of a silica gel rotary desiccant wheel

**Fig. 7** Process and regeneration area of the desiccant wheel

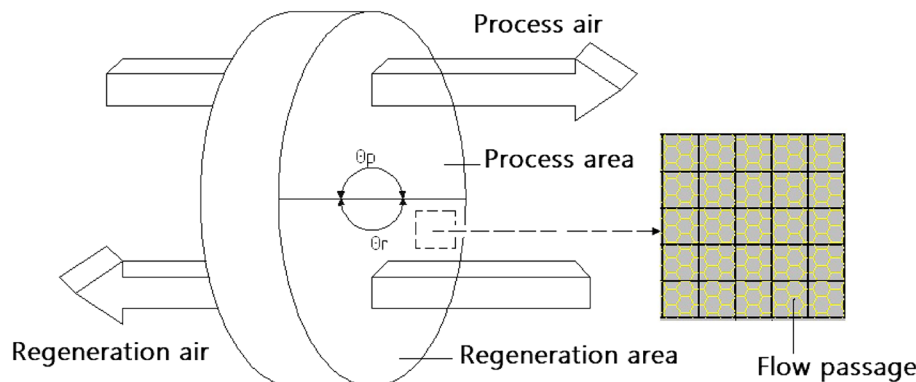


**Table 3** Operating parameters of the rotary desiccant wheel taken for experimentation

Parameters	Parametric variations
Rotational speed, N (rph)	10, 20, 30
Process air flow rate, mp (kg/h)	49, 122
Regeneration air flow rate, mr (kg/h)	49, 122
Sector area of process air, (%)	50, 75
Sector area of regeneration air, (%)	50, 25
Flow type	Parallel and counter
Wheel material	Silica gel, silica gel-lithium chloride, silica gel-molecular sieve 5A, and silica gel-lithium chloride-molecular sieve 5A

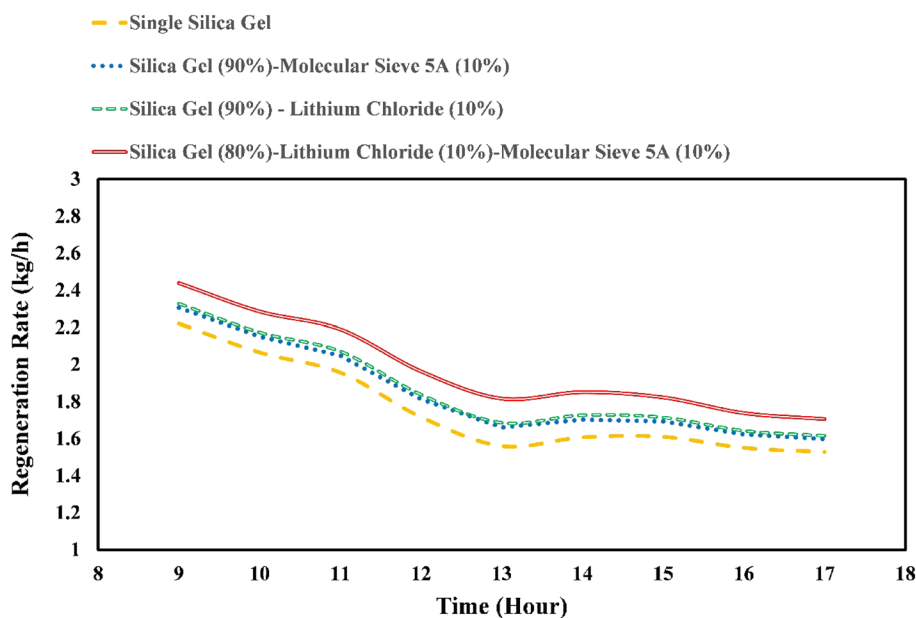
and three composite rotary desiccant wheels at various parameters using a parabolic trough solar collector to regenerate the rotary desiccant wheel. The composite rotary desiccant wheel includes 90% silica gel-10% molecular sieves, 90% silica gel-10% LiCl and 80% silica gel-10% LiCl-10% molecular sieves. These four rotary desiccant wheels (silica gel and three composite rotary desiccant wheels) with mentioned composition percentage are tested to evaluate the adsorption rate and regeneration rate of the rotary desiccant wheel under various combinations. The performance is checked for various rotational speeds, different types of flow arrangements, same and different sector angles and varying regeneration/process (R/P) ratios under various atmospheric conditions. Performance comparison of the different desiccant wheels through this experiment has been carried out in parallel and counter flow arrangement by taking two sets of different sector areas at the process and regeneration sector (adsorption 50% – regeneration 50% and adsorption 75% – regeneration 25%) with

varying rotational speed of the desiccant wheel as well as the varying ratio of mass flow rate (ratio of mass flow rate at regeneration side to process side R/P = 0.4, 2.5 and 1).

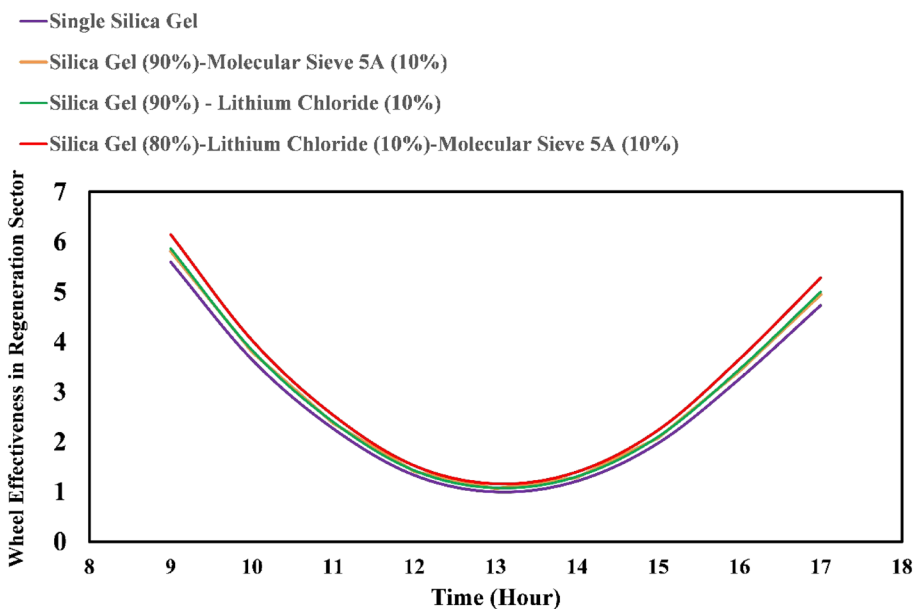
## 5 Discussions

The performance of the silica gel desiccant wheel and other composite desiccant wheels have been separately examined through experiments for adsorption and regeneration processes. The hot air at a temperature range of 52.3–71.3 °C achieved by a parabolic trough collector has been used to regenerate the desiccant wheel. Table 3 shows the operating parameters along with their variations chosen for the present experimentation purpose. The performance comparison for all desiccant wheels has been done by keeping all the operating parameters the same for all the desiccant wheels.

**Fig. 8** Variation of regeneration rate during the daytime



**Fig. 9** Variation of wheel effectiveness in the regeneration sector during the daytime



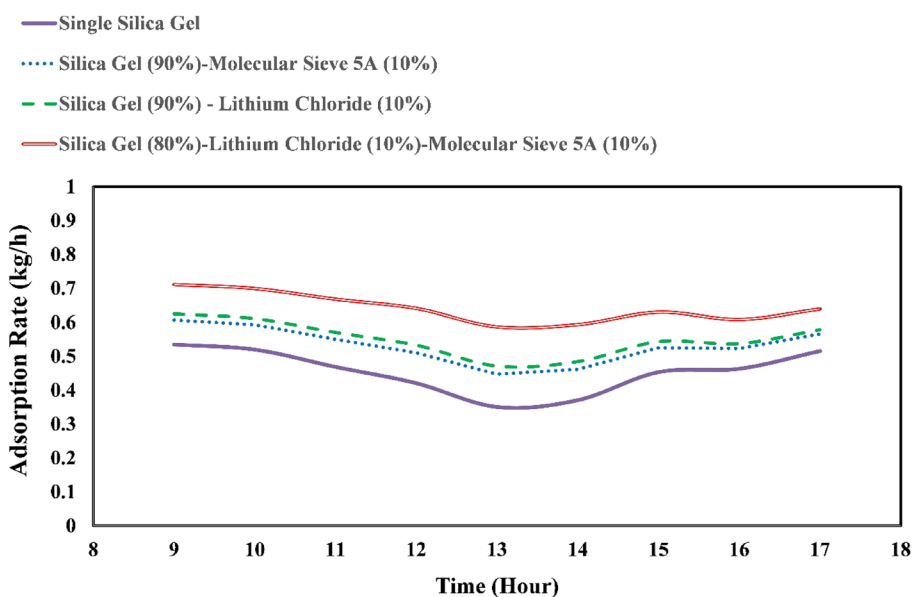
The regeneration rate of the wheels has been presented in Figs. 8 and 9 shows the wheel effectiveness in the regeneration sector.

Figure 8 shows that the regeneration rate of silica gel is the lowest and regeneration of composite desiccant material 80% silica gel-10% LiCl-10% molecular sieves 5A. The highest regeneration rate is obtained in the morning at 09.00 h. From 09.00 to 13.00 h, the regeneration rate decreases and from 13.00 h onward it remains constant.

Since present experiments have been performed throughout the year hence it is difficult to present all the observations made during the complete experimentation. Hence the observation of this experiment performed

on different days for the different desiccant wheels on which wheels show their highest performance has been presented for all important parameters with respect to time. The combination of operating parameters for all the above representations for maximum performance of all the wheels has been found with the rotational speed of 10 rph, process and regeneration flow rate of 122 kg/h, process, and regeneration sector area of 75% and 25%, in counterflow arrangement respectively. From Fig. 9, it is observed that wheel effectiveness in the regeneration sector decreases from 09.00 to 13.00 h and then increases from 13.00 to 17.00 h.

**Fig. 10** Variation of adsorption rate during the daytime



**Fig. 11** Variation of wheel effectiveness in the adsorption sector during the daytime

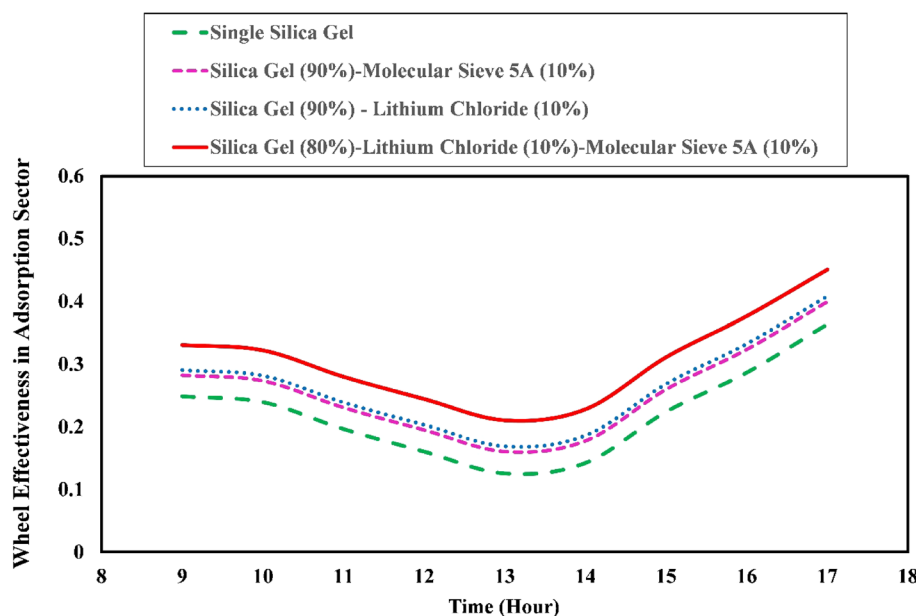


**Table 4** Highest performance of the desiccant wheels

Flow type—counter flow 25% regeneration Speed—10 rph (R/P=1)			Operating parameters			Sector area—75% adsorption Flow rate—122 kg/h	
Composition by mass (%)	Average adsorption rate (kg/h)	Average wheel effectiveness in the adsorption sector	Average regeneration rate (kg/h)	Average wheel effectiveness in the regeneration sector	Percentage improvement of composite desiccant in Average adsorption rate (%)	Percentage improvement of composite desiccant in average regeneration rate (%)	
Silica gel	Molecular sieve 5A	LiCl					
100	0	0	0.46	1.76	2.78	–	
90	10	0	0.53	1.84	2.91	17.45	
90	0	10	0.55	1.87	2.94	21.73	
80	10	10	0.64	1.98	3.11	42.63	

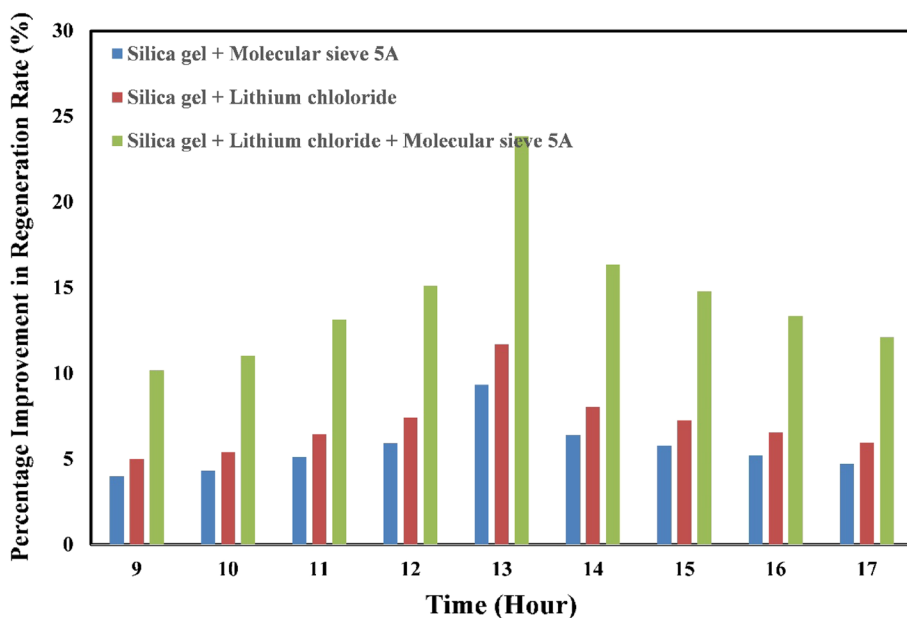
Figure 10 shows that the adsorption rate decreases from 09.00 to 13.00 h and again increases from 13.00 to 17.00 h. Out of all 4-materials adsorption rate is highest for desiccant material silica gel-lithium chloride-molecular sieve 5A.

Figure 11 shows the wheel effectiveness in the adsorption section, which increases from 09.00 to 13.00 h and then increases again. The average value of the several Figs. 8, 9, 10, 11 associated metrics are determined hourly for 1 day (Figs. 10, 11). Table 4 displays the experimental findings of the current study for the average value of adsorption rate, regeneration rate, wheel effectiveness in adsorption sector, wheel effectiveness in regeneration sector, percentage improvement in adsorption rate, and percentage increase in regeneration rate for composite rotary desiccant wheels.

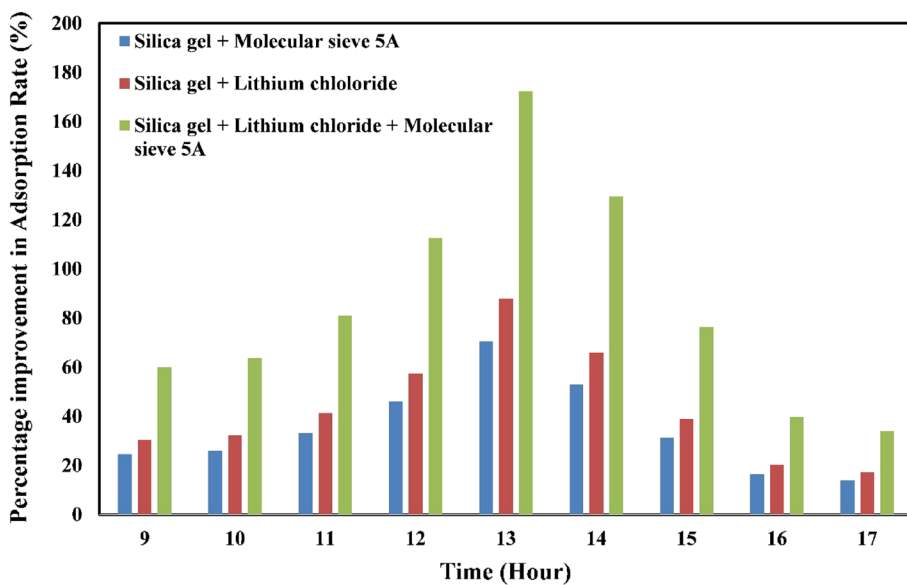
Through this observation, it has been concluded that all composite desiccant wheels show better performance than silica gel desiccant wheel. The silica gel-lithium chloride-molecular sieve 5A desiccant wheel had the greatest performance for all metrics out of all the wheels. At a 122 kg/h airflow rate, the average adsorption and regeneration rates of the silica gel desiccant wheel were 0.46 kg/h and 1.76 kg/h, respectively, whereas 0.64 kg/h and 1.98 kg/h were found for a composite desiccant wheel made from silica gel, lithium chloride, and molecular sieve 5A, respectively, as shown in Table 4.

The maximum adsorption and regeneration rate was reached at 10 rph, while the lowest adsorption and regeneration rate was obtained at 20 rph, according to the results of this experiment (Table 4, Figs. 8, 9, 10, and 11). Figures 12 and 13 illustrate the % improvement in

**Fig. 12** Percentage improvements in regeneration rate of composite desiccant wheels as compared to silica gel desiccant wheel



**Fig. 13** Percentage improvements in adsorption rate of composite desiccant wheels as compared to silica gel desiccant wheel



regeneration and adsorption rates of three composite desiccant wheels over a silica gel desiccant wheel.

Figure 12 shows percentage improvement in regeneration rate of composite desiccant wheel in comparison with plane silica gel. Percentage improvement in regeneration rate for all composite desiccant wheels increases from 09.00 to 13.00 h and then decreases up to 17.00 h. Highest percentage improvement in regeneration rate is shown by composite desiccant made from silica gel-lithium chloride-molecular sieve 5A.

Figure 13 shows a percentage improvement in the adsorption rate of the composite desiccant wheel in comparison with plane silica gel. Percentage improvement

in adsorption rate for all composite desiccant wheels increases from 09.00 to 13.00 h and then decreases up to 17.00 h. The highest percentage improvement in adsorption rate is shown by composite desiccant made silica gel-lithium chloride-molecular sieve 5A.

The desiccant wheel made from silica gel-lithium chloride-molecular sieve 5A had the highest regeneration and adsorption rate of all the desiccant wheels examined, according to all of the data. The (silica gel-lithium chloride-molecular sieve 5A) desiccant wheel has a smaller proportion of silica gel, which results in a better result. The composite desiccant wheel constructed of cellulose had the lowest performance of the

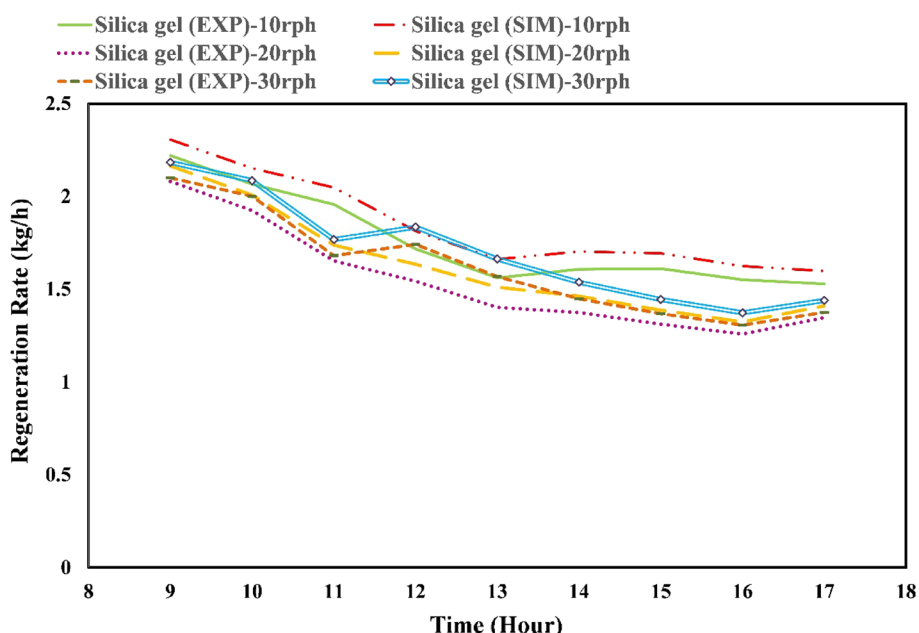
**Table 5** Uncertainty in the performance of the desiccant wheel

Desiccant wheel type	Type of flow	R/P ratio	Wheel speed (rph)	Mass flow rate (kg/h)	Absorption rate ( $R_a$ ) (%)	Regeneration Rate ( $R_r$ ) (%)	Wheel effectiveness in adsorption sector ( $E_a$ ) (%)	Wheel effectiveness in Regeneration sector ( $E_r$ ) (%)
				$m_r$ $m_p$				
Silica gel desiccant wheel	Counter flow	1	10	122   122	4.48	0.71	5.18	0.33
Composite desiccant wheel made from 90% silica gel-10% molecular sieves	Counter flow	1	10	122   122	4.76	0.72	6.07	0.36
Composite desiccant wheel made from 90% silica gel-10% lithium chloride	Counter flow	1	10	122   122	4.73	0.72	5.97	0.36
Composite desiccant wheel made from 80% silica gel-10% lithium chloride-10% molecular sieves	Counter flow	1	10	122   122	4.72	0.71	5.96	0.33

three composite desiccants tested (silica gel-molecular sieve 5A) (Figs. 12, 13). From Figs. 9 and 11 it is observed that wheel effectiveness in the regeneration sector and adsorption sector decreases from 9 to 13 h and increases from 13 to 17 h since relative humidity decreases from 9 to 13 h and increases from 13 to 17 h. Table 5 presents the uncertainty analysis for each of the four types of desiccant wheels in terms of adsorption rate, regeneration

rate, wheel effectiveness in the adsorption sector, and wheel effectiveness in the regeneration sector.

It is observed that uncertainty varies from 4.48 to 4.76% in the adsorption rate, 0.71–0.72% in the regeneration rate, 5.18–6.07% in wheel effectiveness in the adsorption sector and 0.33–0.36% in wheel effectiveness in the regeneration sector.

**Fig. 14** Variation of regeneration rate for experimental and simulation results

**Fig. 15** Variation of wheel effectiveness in the regeneration sector for experimental and simulation results

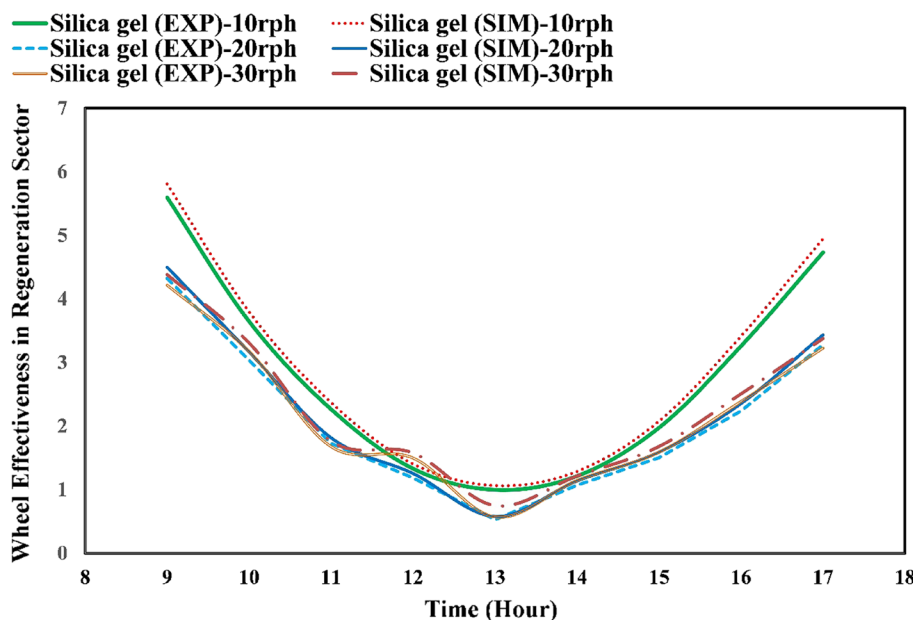
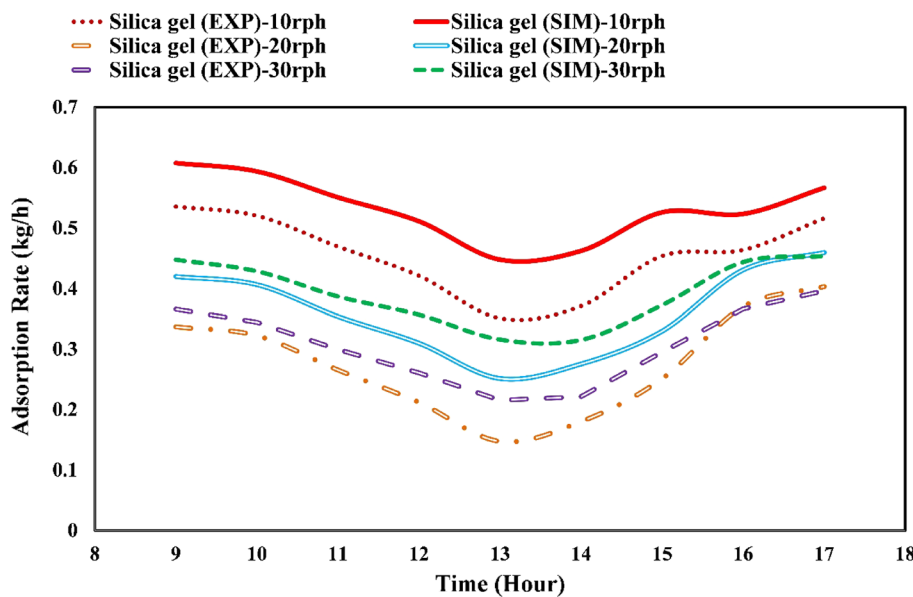


**Fig. 16** Variation of adsorption rate for experimental and simulation results



## 6 Validation

NovelAire technology desiccant wheel simulation software was used to confirm the experimental results for the silica gel desiccant wheel [49]. In this validation, the regeneration and adsorption rates of a silica gel desiccant wheel used to produce dry air were compared to experimental studies. The computational and experimental findings of the silica gel desiccant wheel are compared for various

rotational speeds, counterflow arrangements, sectors, and R/P ratios. Figures 14, 15, 16, and 17 compare experimental and simulation findings for a silica gel desiccant wheel, whereas Table 6 illustrates the performance characteristics of a silica gel desiccant wheel for simulation purposes.

The governing equations used by software are shown by Eqs. 10 and 11.

The mass conservation in the air can be expressed as [49]:

**Fig. 17** Variation of wheel effectiveness in the adsorption sector for experimental and simulation results

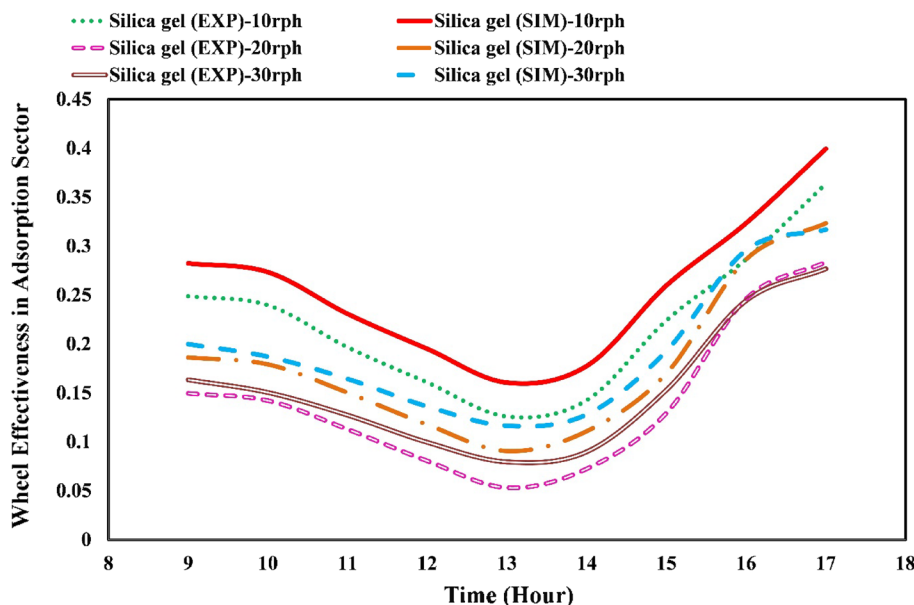


**Table 6** Performance parameters of the desiccant wheel for unequal sector area

Parameters	Quantity
Material	Silica gel
The rotational speed of the desiccant wheel, N (rph)	10, 20, 30
Process air flow rate, $M_p$ , (kg/h)	122
Regeneration air flow rate, $M_r$ (kg/h)	122
Process air sector area, (%)	75
Regeneration air sector area, (%)	25
Flow type	Counterflow

$$\rho_{da}A \left( \frac{\partial W_a}{\partial t} + v \frac{\partial W_a}{\partial x} \right) = h_m P_e (W_a - W_d) \quad (10)$$

The mass conservation in desiccant is given by:

$$\begin{aligned} & \varepsilon(1 - A_r) A_t dx \rho_{da} \frac{\partial W_d}{\partial t} + (1 - \varepsilon)(1 - A_r) A_t \emptyset dx \rho_d \frac{\partial dw}{\partial t} \\ &= \rho_d (1 - \varepsilon) (1 - A_r) A_t \emptyset D_s \frac{\partial^2 dw}{\partial x^2} \\ &+ \rho_{da} \varepsilon (1 - A_r) A_t D_{comb} \frac{\partial^2 W_d}{\partial x^2} + h_m P_e dx (W_a - W_d) \end{aligned} \quad (11)$$

Figure 14 shows the comparison of the regeneration rate of experimental and simulation results of silica gel for 10, 20, and 30 rph. From this it is observed that the simulation result of silica gel at 10 rph has the highest regeneration rate.

Figure 15 shows the comparison of wheel effectiveness in the regeneration sector for experimental and simulation results of silica gel for 10, 20, and 30 rph. From this it is observed that the simulation result of silica gel at 10 rph has the highest wheel effectiveness in the regeneration sector.

The percentage deviation between experimental results, and simulation results for the silica gel desiccant wheel is presented in Table 7.

Figure 16 shows the comparison of the adsorption rate of experimental and simulation results of silica gel

**Table 7** Percentage deviation in experimental and simulation results

Parameters	10 rph			20 rph			30 rph		
	Exp	Sim	% Deviation	Exp	Sim	% Deviation	Exp	Sim	% Deviation
Average regeneration rate (kg/h)	1.75	1.84	4.70	1.54	1.62	5.09	1.62	1.70	4.82
Average wheel effectiveness in the regeneration sector	2.77	2.90	4.41	2.09	2.20	4.73	2.16	2.28	5.25
Average adsorption rate (kg/h)	0.45	0.53	14.35	0.27	0.35	23.09	0.30	0.39	21.45
Average wheel effectiveness in the adsorption sector	0.22	0.25	13.62	0.14	0.17	21.33	0.15	0.19	20.35

**Table 8** Operating parameters of the desiccant wheel for counter flow and different sector angles (parameters at best performance)

Parameters	Quantity
Material	Silica gel
Rotational speed, N (rph)	10
Airflow rate of process air, $m_p$ (kg/h)	122
Airflow rate of regeneration air, $m_r$ (kg/h)	122
Sector angle of process air, $\theta_p$ (°)	270°
Sector angle of regeneration air, $\theta_r$ (°)	90°
Flow type	Counterflow

for 10, 20, and 30 rph. From this is it observed that the simulation result of silica gel at 10 rph has the highest adsorption rate.

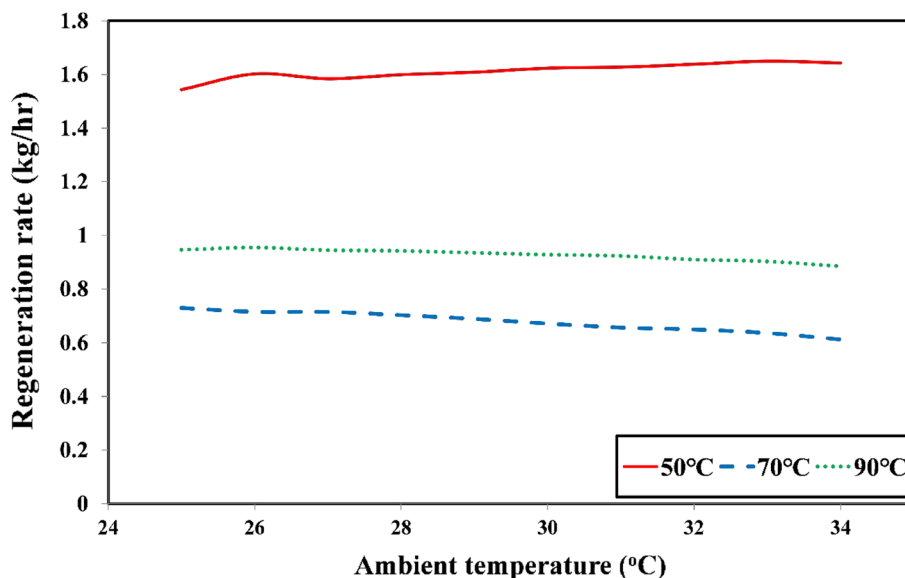
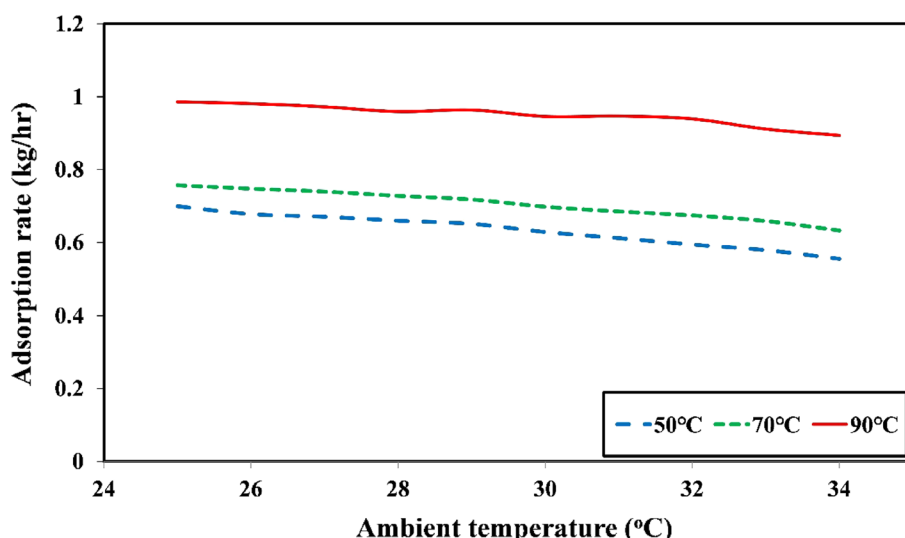
**Fig. 18** Variation of regeneration rate at various regeneration temperatures**Fig. 19** Variation of adsorption rate at various regeneration temperatures

Figure 17 shows the comparison of wheel effectiveness in the adsorption sector for experimental and simulation results of silica gel for 10, 20, and 30 rph. From this is it observed that the simulation result of silica gel at 10 rph has the highest wheel effectiveness in the adsorption sector.

The similar atmospheric conditions as the experimental setup were given as input to the NovelAire software for the simulation purpose and the average value of various parameters available in Table 7 are calculated for a single day on an hourly basis. Through this observation, it is observed that experimental results show close agreements with simulation results (Table 6, Figs. 14, 15, 16, and 17).

## 7 Simulation at various conditions

Additional to the present experimental study and with proper validation some simulation work has been carried out to observe the effects of some important operating parameters on the regeneration rate and adsorption rate of silica gel desiccant wheel. Table 8 shows the various operating parameters related to this simulation study.

### 7.1 Effect of regeneration temperatures on regeneration rate

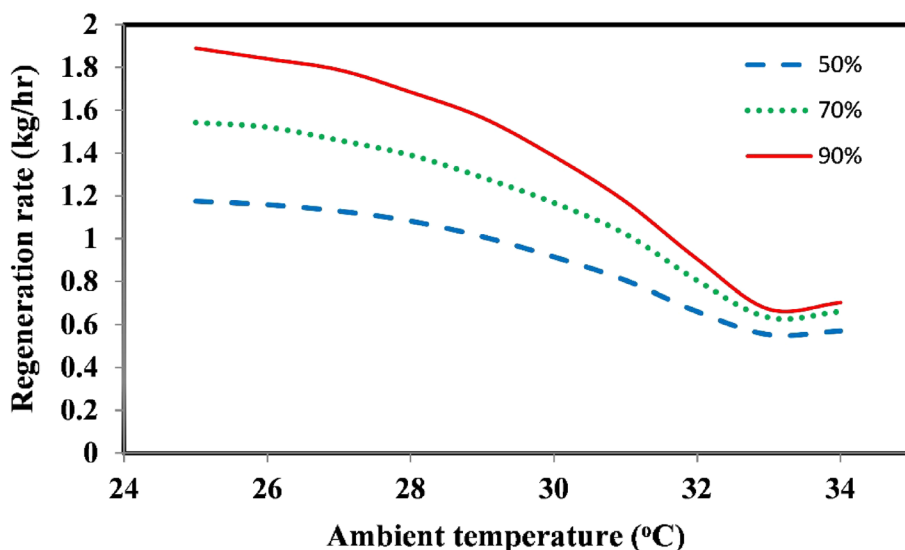
The effect of regeneration temperatures on regeneration rate has been observed at three temperatures i.e., 50 °C, 70 °C, and 90 °C in Fig. 18.

It exhibits that, the regeneration rate is highest at the lowest regeneration temperature whereas it is the lowest with intermediate regeneration temperature i.e., 70 °C. One more observation that has been made through this simulation is that at the lowest regeneration temperature, the regeneration rate increases slightly with the increase of ambient temperature, whereas for the other two regeneration temperature regeneration rate decreases as the ambient temperature increases (Fig. 18).

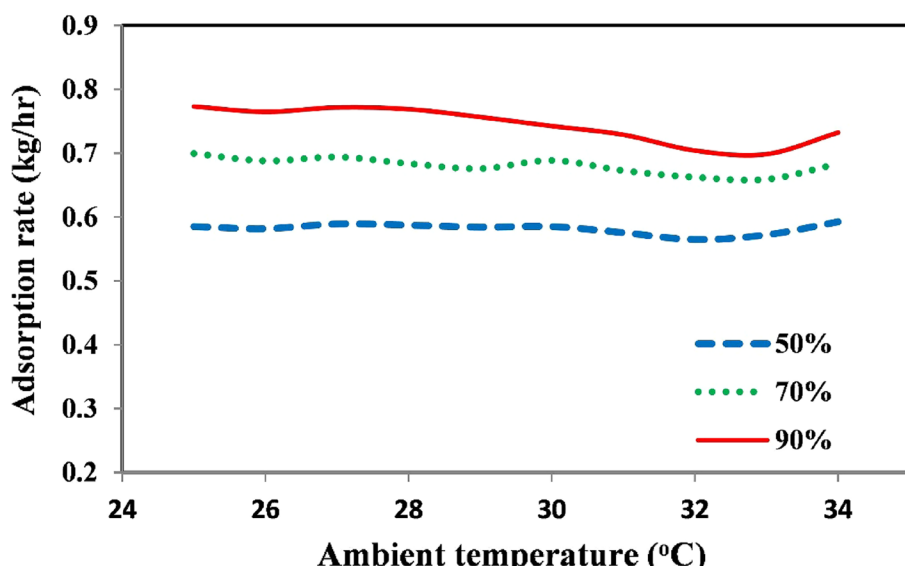
### 7.2 Effect of regeneration temperatures on adsorption rate

Figure 19 shows the variation in adsorption rate at various regeneration temperatures. Similar to the previous study

**Fig. 20** Variation of regeneration rate at a various relative humidity



**Fig. 21** Variation of adsorption rate at a various relative humidity



the effect of regeneration temperatures on the adsorption rate has been analyzed at three temperatures i.e., 50 °C, 70 °C, and 90 °C.

It was found that as the regeneration temperature rises, so does the adsorption rate. Moreover, at all three regeneration temperatures adsorption rate decreases slightly with the increase in ambient temperature (Fig. 19).

The desorption properties of the desiccant material are primarily responsible for the phenomenon of a lower regeneration rate at higher regeneration temperatures in desiccant-based systems, such as desiccant wheels.

### 7.3 Effect of relative humidity on regeneration rate

In this simulation, the effect of relative humidity has been examined for the regeneration rate (shown in Fig. 20). Three values of relative humidity have been considered with an ambient temperature range of 24–34 °C.

Through this simulation, it has been observed that as the relative humidity increases regeneration rate also increases, and with the increase of ambient temperature, the regeneration rate decreases significantly (Fig. 20). It shows that, regeneration rate increases as the

regeneration temperature increases. As the ambient temperature increases regeneration rate decreases.

### 7.4 Effect of relative humidity on adsorption rate

The effect of relative humidity has been simulated to measure its effect on adsorption rate, through the variation in ambient temperature. This simulation results with Fig. 21 show that as the relative humidity increases, the adsorption rate also increases.

The above simulation results related to various ambient conditions can be summarized as the ambient temperature increases regeneration rate and adsorption rate decreases since ambient air with high temperature has a high affinity to hold moisture, which is responsible for the decrease in adsorption and regeneration rate (Fig. 21). It shows that, adsorption rate increases as the regeneration temperature increases.

**Fig. 22** Comparison of present work with published work for wheel effectiveness in the adsorption sector

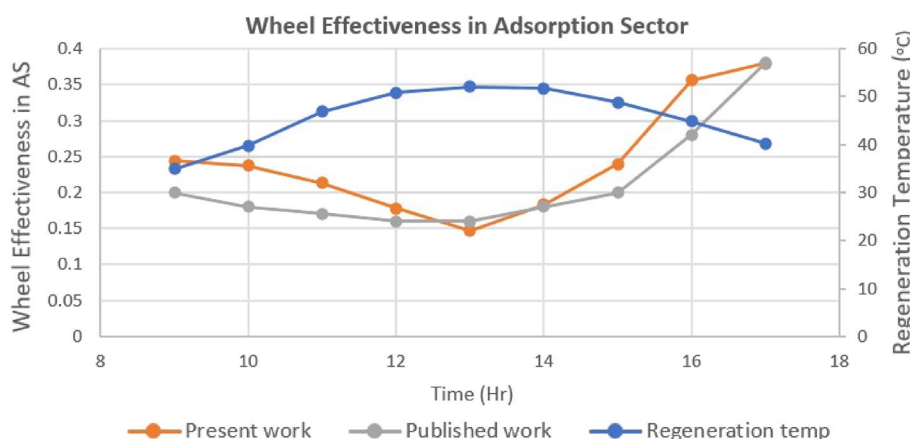
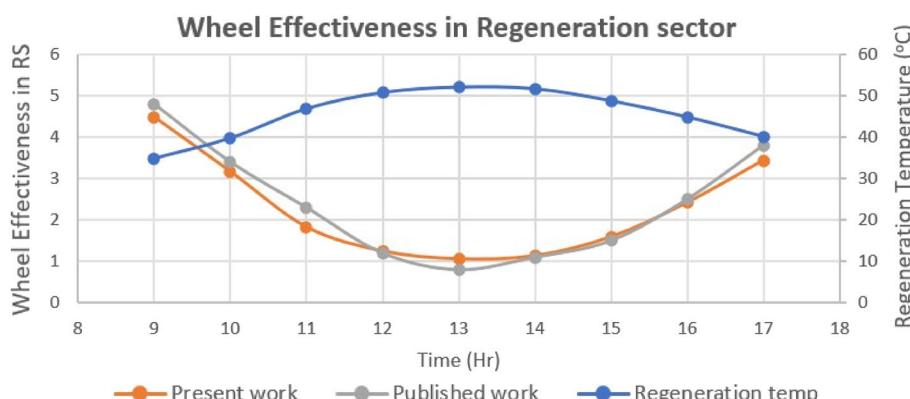


**Fig. 23** Comparison of present work with published work for wheel effectiveness in the regeneration sector



## 8 Comparison with published work

Comparing the findings of our current research with the previously published study by Avadhesh Yadav and V. K. Bajpai titled "The performance of solar powered desiccant dehumidifier in India: an experimental investigation" poses a significant challenge due to the inherent variability of key parameters. These parameters include ambient temperature, regeneration temperature, solar intensity, mass flow rate of air, and time, all of which are difficult to maintain at identical levels across different experimental setups.

Nonetheless, despite these challenges, we have endeavored to draw meaningful comparisons between our work and the aforementioned study. Specifically, we have focused our attention on the analysis of the wheel effectiveness in both the adsorption sector and the regeneration sector of the desiccant dehumidifier (shown in Figs. 22 and 23) [50].

Upon thorough examination, we have observed a noteworthy correspondence between the graphs depicting wheel effectiveness in the adsorption sector and during the regeneration process. This alignment in the graphical representation implies a certain degree of similarity in the performance trends of the desiccant dehumidification process between our present research and the work conducted by Avadhesh Yadav and V. K. Bajpai. While the broader contextual differences in experimental conditions prevent a direct one-to-one comparison, this observed congruence in wheel effectiveness profiles encourages further exploration and analysis.

Present work	Published work
Material: silica gel	Material: silica gel
Flow: parallel	Flow: parallel
Sector angle: 180°	Sector angle: 180°
Wheel speed: 20 RPH	Wheel speed: 23 RPH

- (a) Wheel effectiveness in the adsorption sector.  
See Fig. 22.
- (b) Wheel effectiveness in the regeneration sector.  
See Fig. 23.

## 9 Conclusions

In this work, the primary objective was to assess the performance of different composite desiccant wheels for air dehumidification and to explore the impact of various operational parameters on their adsorption and

regeneration rates. Specifically, aimed to compare the effectiveness of silica gel desiccant wheels with a composite of silica gel, lithium chloride, and molecular sieve 5A.

Investigation yielded several significant insights. Notably, we observed that all selected composite desiccant wheels, including the combination of silica gel, lithium chloride, and molecular sieve 5A, exhibited their optimal performance in a counterflow arrangement. This was particularly evident when employing a regeneration area of 25% and an adsorption area of 75%, with a process and regeneration flow rate of 122 kg/h ( $R/P = 1$ ) and a desiccant wheel speed of 10 rph.

Among the various desiccant wheel configurations, the composite of silica gel, lithium chloride, and molecular sieve 5A demonstrated the best adsorption and regeneration rates. Conversely, the silica gel desiccant wheel exhibited the lowest rates in both aspects. Notably, our experimental results for the silica gel desiccant wheel aligned well with simulation data, enhancing the credibility of our findings.

In addition to the above experimental study and its validation, some simulation work has been carried out to observe the effects of some important operating parameters on the regeneration rate and adsorption rate of the silica gel desiccant wheel.

Some other significant findings of this experimental work are listed below:

The average adsorption and regeneration rate of the silica gel desiccant wheel was found to be 0.46 kg/h and 1.76 kg/h.

The average adsorption and regeneration rates of the composite desiccant wheel composed of silica gel, lithium chloride, and molecular sieve 5A were 0.64 kg/h and 1.98 kg/h, respectively.

The average percent improvement in adsorption rate and regeneration rate of composite desiccant wheel silica gel-molecular sieve 5A, silica gel-lithium chloride, and silica gel-lithium chloride-molecular sieve 5A over silica gel desiccant wheel are 17.45%, 21.73%, 42.63%, and 5.01%, 6.29%, 12.81% respectively.

The maximum percent deviation in regeneration rate for the experimental study as compared to the simulation study was found to be 4.82% during wheel speed of 30 rph.

The maximum percent deviation in adsorption rate for the experimental study as compared to the simulation study was found to be 21.45% during wheel speed of 30 rph.

This investigation can be replicated utilizing various permutations of composite desiccant wheels to assess the efficacy of desiccant materials in enhancing air quality.

**Author contributions** Actual study, conception, design, material preparation, data collection and analysis were performed by KSR, PVW, VPK, VWK, YN, and RJ and review of the manuscript was performed by MAK and MM.

**Funding** No funding was received for this work.

**Data availability** The data that support the findings of this study are available on request from the Kishor S. Rambhad. The data are not publicly available.

## Declarations

**Conflict of interest** There is no conflict of interest.

**Open Access** This article is licensed under a Creative Commons Attribution 4.0 International License, which permits use, sharing, adaptation, distribution and reproduction in any medium or format, as long as you give appropriate credit to the original author(s) and the source, provide a link to the Creative Commons licence, and indicate if changes were made. The images or other third party material in this article are included in the article's Creative Commons licence, unless indicated otherwise in a credit line to the material. If material is not included in the article's Creative Commons licence and your intended use is not permitted by statutory regulation or exceeds the permitted use, you will need to obtain permission directly from the copyright holder. To view a copy of this licence, visit <http://creativecommons.org/licenses/by/4.0/>.

## References

1. Gommed K, Grossman G (2004) A liquid desiccant system for solar cooling and dehumidification. *J Sol Energy Eng Trans ASME* 126:875–885. <https://doi.org/10.1115/1.1690284>
2. Shamim JA, Hsu WL, Paul S, Yu L, Daigui H (2021) A review of solid desiccant dehumidifiers: current status and near-term development goals in the context of net zero energy buildings. *Renew Sustain Energy Rev* 137:110456. <https://doi.org/10.1016/j.rser.2020.110456>
3. Das A, Das RS, Das K (2022) Performance analysis of aqueous LiCl and CaCl<sub>2</sub> based falling film dehumidifier with surface modification. *Appl Therm Eng* 200:117704. <https://doi.org/10.1016/j.applthermaleng.2021.117704>
4. Daou K, Wang RZ, Xia ZZ (2006) Desiccant cooling air conditioning: a review. *Renew Sustain Energy Rev* 10(2):55–77. <https://doi.org/10.1016/j.rser.2004.09.010>
5. Lee Y, Park S, Kang S (2021) Performance analysis of a solid desiccant cooling system for a residential air conditioning system. *Appl Therm Eng* 182:116091. <https://doi.org/10.1016/j.applthermaleng.2020.116091>
6. Waugaman DG, Kini A, Kettleborough CF (1993) A review of desiccant cooling systems. *J Energy Resour Technol* 115(1):1–8. <https://doi.org/10.1115/1.2905965>
7. Jia CX, Dai YJ, Wu JY, Wang RZ (2006) Experimental comparison of two honeycombed desiccant wheels fabricated with silica gel and composite desiccant material. *Energy Convers Manag* 47:2523–2534. <https://doi.org/10.1016/j.enconman.2005.10.034>
8. Ramzy A, Abdelmeguid H, Elawady WM (2015) A novel approach for enhancing the utilization of solid desiccants in packed bed via intercooling. *Appl Therm Eng* 78:82–89. <https://doi.org/10.1016/j.applthermaleng.2014.12.035>
9. Hamed AM, Abd El Rahman WR, El-Eman SH (2010) Experimental study of the transient adsorption/desorption characteristics of silica gel particles in fluidized bed. *Energy* 35:2468–2483. <https://doi.org/10.1016/j.energy.2010.02.042>
10. Abd-Elhady MM, Salem MS, Hamed AM, El-Sharkawy II (2022) Solid desiccant-based dehumidification systems: a critical review on configurations, techniques, and current trends. *Int J Refrig* 133:337–352. <https://doi.org/10.1016/j.ijrefrig.2021.09.028>
11. Lai L, Wang X, Kefayati G, Hu E (2021) Evaporative cooling integrated with solid desiccant systems: a review. *Energies* 14(18):5982. <https://doi.org/10.3390/en14185982>
12. Wu XN, Ge TS, Dai YJ, Wang RZ (2018) Review on substrate of solid desiccant dehumidification system. *Renew Sustain Energy Rev* 82:3236–3249. <https://doi.org/10.1016/j.rser.2017.10.021>
13. Rippy KC, Volk E (2022) Corrosion of metal alloys in potassium acetate solutions for liquid desiccant dehumidification and air conditioning. *Energies* 15(12):4421. <https://doi.org/10.3390/en15124421>
14. Wrobel J, Morgenstern P, Schmitz G (2013) Modeling and experimental validation of the desiccant wheel in a hybrid desiccant air conditioning system. *Appl Therm Eng* 51:1082–1091. <https://doi.org/10.1016/j.applthermaleng.2012.09.033>
15. Liu S, Jeong C-H, Yeo M-S (2020) Effect of evaporator position on heat pump assisted solid desiccant cooling systems. *Energies* 13(22):5918. <https://doi.org/10.3390/en13225918>
16. Jani DB, Mishra M, Sahoo PK (2016) Solid desiccant air conditioning—a state of the art review. *Renew Sustain Energy Rev* 60:1451–1469. <https://doi.org/10.1016/j.rser.2016.03.031>
17. Tretiak CS, Ben Abdallah N (2009) Sorption and desorption characteristics of a packed bed of clay–CaCl<sub>2</sub> desiccant particles. *Sol Energy* 83:1861–1870. <https://doi.org/10.1016/j.solener.2009.06.017>
18. Alahmer A, Alsaqoor S, Borowski G (2019) Effect of parameters on moisture removal capacity in the desiccant cooling systems. *Case Stud Therm Eng* 13:100364. <https://doi.org/10.1016/j.csite.2018.11.015>
19. Jia CX, Dai YJ, Wu JY, Wang RZ (2006) Analysis on a hybrid desiccant air-conditioning system. *Appl Therm Eng* 26:2393–2400. <https://doi.org/10.1016/j.applthermaleng.2006.02.016>
20. Kabeel AE (2007) Solar powered air conditioning system using rotary honeycomb desiccant wheel. *Renew Energy* 32:1842–1857. <https://doi.org/10.1016/j.renene.2006.08.009>
21. Chen CH, Hsu CY, Chen CC, Chiang YC, Chen SL (2016) Silica gel/polymer composite desiccant wheel combined with heat pump for air-conditioning systems. *Energy* 94:87–99. <https://doi.org/10.1016/j.energy.2015.10.139>
22. Chen CH, Hsu CY, Chen CC, Chen SL (2015) Silica gel polymer composite desiccants for air conditioning systems. *Energy Build* 101:122–132. <https://doi.org/10.1016/j.enbuild.2015.05.009>
23. Tretiak CS, Ben Abdallah N (2009) Sorption and desorption characteristics of a packed bed of clay–CaCl<sub>2</sub> desiccant particles. *Sol Energy* 83:1861–1870. <https://doi.org/10.1016/j.solener.2009.06.017>
24. Ramzy K A, Kadoli R, Ashok Babu TP (2011) Improved utilization of desiccant material in packed bed dehumidifier using composite particles. *Renew Energy* 36:732–742. <https://doi.org/10.1016/j.renene.2010.06.038>
25. Chua KJ, Islam MR (2015) Experimental study of composite dessicants for energy efficient air dehumidification. *IIUM Eng. J* 16:1–11. <https://doi.org/10.31436/iiumej.v16i2.600>
26. Zhang LZ, Fu HX, Yang QR, Xu JC (2014) Performance comparisons of honeycomb-type adsorbent beds (wheels) for air dehumidification with various desiccant wall materials. *Energy* 65:430–440. <https://doi.org/10.1016/j.energy.2013.11.042>

27. Majumdar P (1998) Heat and mass transfer in composite desiccant pore structures for dehumidification. *Sol Energy* 62:1–10. [https://doi.org/10.1016/S0038-092X\(97\)00080-7](https://doi.org/10.1016/S0038-092X(97)00080-7)
28. Jia CX, Dai YJ, Wu JY, Wang RZ (2007) Use of compound desiccant to develop high performance desiccant cooling system. *Int J Refrig* 30:345–353. <https://doi.org/10.1016/j.ijrefrig.2006.04.001>
29. Zhang XJ, Dai YJ, Wang RZ (2003) A simulation study of heat and mass transfer in a honeycombed rotary desiccant dehumidifier. *Appl Therm Eng* 23:989–1003. [https://doi.org/10.1016/S1359-4311\(03\)00047-4](https://doi.org/10.1016/S1359-4311(03)00047-4)
30. Zhang XJ, Sumathy K, Dai YJ, Wang RZ (2006) Dynamic hygroscopic effect of the composite material used in desiccant rotary wheel. *Sol Energy* 80:1058–1061. <https://doi.org/10.1016/j.solener.2005.07.008>
31. Motaghian S, Rayegan S, Pasdarshahri H, Ahmadi P, Rosen MA (2021) Comprehensive performance assessment of a solid desiccant wheel using an artificial neural network approach. *Int J Heat Mass Transf* 165:120657. <https://doi.org/10.1016/j.ijheatmasstransfer.2020.120657>
32. Liu Z, Cheng C, Han J, Zhao Z, Qi X (2022) Experimental evaluation of the dehumidification performance of a metal organic framework desiccant wheel. *Int J Refrig* 133:157–164. <https://doi.org/10.1016/j.ijrefrig.2021.09.033>
33. Goodarzia G, Thirukonda N, Heidari S, Akbarzadeh A, Date A (2017) Performance evaluation of solid desiccant wheel regenerated by waste heat or renewable energy. *Energy Procedia* 110:434–439. <https://doi.org/10.1016/j.egypro.2017.03.165>
34. Chen L, Tan Y (2020) The performance of a desiccant wheel air conditioning system with high-temperature chilled water from natural cold source. *Renew Energy* 146:2142–2157. <https://doi.org/10.1016/j.renene.2019.08.082>
35. Ali M, Habib MF, Ahmed Sheikh N, Akhter J, UI SI, Gilani H (2022) Experimental investigation of an integrated absorption-solid desiccant air conditioning system. *Appl Therm Eng* 203:117912. <https://doi.org/10.1016/j.applthermaleng.2021.117912>
36. Samad A, Waheed A, Bilal M, Fatima M, Zahra A, Siddiqui MS (2020) Dynamic simulation and parametric analysis of solar assisted desiccant cooling system with three configuration schemes. *Sol Energy* 197:22–37. <https://doi.org/10.1016/j.solener.2019.12.076>
37. Valarezo AS, Sun XY, Ge TS, Dai YJ, Wang RZ (2019) Experimental investigation on performance of a novel composite desiccant coated heat exchanger in summer and winter seasons. *Energy* 166:506–518. <https://doi.org/10.1016/j.energy.2018.10.092>
38. Li X, Chen J, Sun X, Zhao Y, Chong C, Dai Y, Wang CH (2021) Multi-criteria decision making of biomass gasification-based cogeneration systems with heat storage and solid dehumidification of desiccant coated heat exchangers. *Energy* 233:121–122. <https://doi.org/10.1016/j.energy.2021.121122>
39. Vivekh P, Bui DT, Kumja M, Islam MR, Chua KJ (2019) Theoretical performance analysis of silica gel and composite polymer desiccant coated heat exchangers based on a CFD approach. *Energy Convers Manag* 187:423–446. <https://doi.org/10.1016/j.enconman.2019.02.093>
40. Rambhad K, Jondhale P, Kambale R, Jedhe V, Thakare K (2021) CFD analysis of solid desiccant dehumidifier wheel. *Int J Anal Exp Finite Elem Anal* 8(1):12–20. <https://doi.org/10.26706/ijaefea.1.8.20210302>
41. Srivastava S, Yadav A (2018) Water generation from atmospheric air by using composite desiccant material through fixed focus concentrating solar thermal power. *Sol Energy* 169:302–315. <https://doi.org/10.1016/j.solener.2018.03.089>
42. Liu M, Tu R, Wu Z, Zhu J (2022) Performance analyses of desiccant wheel-assisted atmospheric water harvesting system using renewable heating and cooling sources. *Energy Convers Manag* 252:115065. <https://doi.org/10.1016/j.enconman.2021.115065>
43. Rambhad KS, Walke PV, Tidke DJ (2016) Solid desiccant dehumidification and regeneration methods—a review. *Renew Sustain Energy Rev* 59:73–83. <https://doi.org/10.1016/j.rser.2015.12.264>
44. Rambhad KS, Walke PV (2018) Regeneration of composite desiccant dehumidifier by parabolic trough solar collector: an experimental investigation. *Mater Today Proc* 5(11):24358–24366. <https://doi.org/10.1016/j.matpr.2018.10.231>
45. Yadav A, Bajpai VK (2011) Optimization of operating parameters of desiccant wheel for rotation speed. *Int J Adv Sci Technol* 32:109–116
46. Walke PV, Phadke PC, Rambhad KS (2018) Performance evaluation of forced convection desiccant bed solar dryer integrated with sensible heat storage material. *Int J Anal Exp Finite Elem Anal* 2(5):24–35. <https://doi.org/10.26706/IJAEEA.2.5.20180501>
47. Arnoldsoon J (2000) Adsorption Chillers—uptake of ethanol on type RD silica gel. *Institutionen för ekonomisk och industriell utveckling Avdelning: Energisystem*
48. Hu LM, Ge TS, Jiang Y, Wang RZ (2015) Performance study on composite desiccant material coated fin-tube heat exchangers. *Int J Heat Mass Transf* 90:109–120. <https://doi.org/10.1016/j.ijheatmasstransfer.2015.06.033>
49. NovelAire technology desiccant wheel simulation software (2022). <https://www.novelaire.com/desiccant-wheels-31505.html>
50. Yadav A, Bajpai VK (2013) The performance of solar powered desiccant dehumidifier in India: an experimental investigation. *Int J Sustain Eng* 6(3):239–257. <https://doi.org/10.1080/19397038.2012.707252>

**Publisher's Note** Springer Nature remains neutral with regard to jurisdictional claims in published maps and institutional affiliations.